

EMERGING TECH CONFERENCE – Edge Intelligence

Volume 01, 2022, Page 62 – 71

**Proceedings of Emerging Tech Conference:
Edge Intelligence 2022**

Quantification of Muscle Thickness in Gastrocnemius ultrasound images with deep learning

Katakis Sofoklis^{a,*}, Barotsis Nikolaos^b, Kakotaritis Alexandros^a, Economou George^a,
Panagiotopoulos Elias^c, Panayiotakis George^b

^aElectronics Laboratory, Department of Physics, University of Patras, 26504 Patras, Greece

^bDepartment of Medical Physics, School of Medicine, University of Patras, 26504 Patras, Greece

^cOrthopaedic and Rehabilitation Department, Patras University Hospital, 26504 Patras, Greece

katakis.s@upnet.gr

Abstract

The automatic extraction of muscle thickness is an important application in the clinical routine that has been studied extensively in recent years. Following this trend, the well-established UNet and other state-of-the-art convolutional neural networks are assessed for automating this task. A two-step approach is presented to extract the muscle thickness. As the first step, different segmentors are incorporated to delineate the deep and superficial aponeurosis effortlessly. Afterwards, the muscle thickness is calculated by taking the average distance between the two aponeuroses at different muscle points. The examined dataset to evaluate this method consists of ultrasound images of gastrocnemius medialis of 116 young and healthy subjects of different sex. Regarding the results, the deep learning architectures used in this study have achieved similar to human-level performance. In particular, an overall discrepancy between the automatic and the manual muscle thickness measurements equal to 0.11 mm is reported, a significant result that demonstrates the feasibility of automating this task. Furthermore, the Bland-Altman analysis of the measurements exhibits no systematic errors since most differences fall between the 95% limits of agreement. Finally, the two readings have a 0.99 Pearson's correlation coefficient ($p < 0.001$, validation set) and the ICC (2, 1) has surpassed 0.99, showing the reliability of this approach.

1. Introduction

Musculoskeletal ultrasonography (MSK-US) has proven effective in assessing skeletal muscle structure [1] and provides multiple advantages relevant to other medical image modalities. Specifically, it is a non-invasive, safe, portable, low cost examination that provides a detailed imaging of the human muscles. An important application of MSK-US in clinical routine is the muscle thickness measurement due to its correlation with specific muscle disorders. In particular, muscle hypertrophy [2], disuse atrophy [3], ageing [4,5] and pathological conditions [6] have been reported to affect muscle thickness. Furthermore, more recently, in [7], the relation of sarcopenia (a common disease in the elderly) with muscle thickness was studied in the head, neck, upper and lower limb muscles for using this measurement as a potential diagnostic tool.

However, for the operator to perform the measurement, the visual identification of the deep and superficial aponeuroses is needed. The above is a time-consuming task that requires specialised knowledge and multiple years of experience, thus making it user-dependent and error prone. For this reason, different types of software have emerged in recent years to standardise and automate these measurements and to assist the doctor in clinical practice [8–12]. In particular, in [12], Muscle Ultrasound Analysis (MUSA) is proposed, a framework that delineates the deep and superficial aponeuroses with gradient- based filtering. Afterwards, the muscle thickness and pennation angle measurements are extracted with a heuristic approach. Notably, this study revealed the feasibility of automating these measurements using machine learning techniques. However, their approach's downside is that it is based exclusively on gradient-based filtering, which can be error-prone in low- contrast images, a common characteristic of ultrasound recordings of muscles suffering from neuromuscular conditions.

In [13], a deep learning approach was used to automatically extract the muscle thickness, fascicle length and pennation angle from ultrasound longitudinal scans of three different muscles to tackle the difficulties in low contrast images. The authors utilised Attention-UNet [14] to initially segment the deep and superficial aponeuroses and then the measurements were extracted by incorporating a heuristic-based approach. This study can be seen as an extension of the [13], where different deep learning topologies are used to extract muscle thickness in ultrasound images of gastrocnemius medialis. Since the deep and superficial aponeurosis is extracted, the muscle thickness can be calculated by taking the average distance between the two aponeuroses at several muscle points. The main aim of this study is to improve the existing software by introducing state-of-the-art deep learning techniques for calculating, important for diagnostic purposes muscle characteristics, in a better and more reliable way. Such improvement would be of high value since it will allow ultrasonographers to calculate muscle thickness faster, more accurately and in a more standardised fashion.

2. Methods & Materials

2.1 Database

The database used in this study consists of ultrasound recordings of gastrocnemius medialis (GCM) of 116 young and healthy volunteers (49 males and 67 females with a mean age of 25.33 ± 4.92 y) also presented in [15–17]. The ultrasound examinations were performed using a Logiq P9 ultrasound system (GE Healthcare GmbH, Freiburg, Germany) along with a ML6-15 linear array transducer, operating at 10-MHz frequency. All image optimisation modes were switched off to avoid alteration of image characteristics by software processing, except for harmonic tissue imaging. In addition, the gain was set to 50, the dynamic range at 66dB and both were kept constant throughout the examination of all subjects. In Table 1, the demographic characteristics of the dataset are demonstrated.

Subjects	116
Examinations	155
Age (years)	25.33 ± 4.92
Sex (M/F)	49 / 67
Weight (kg)	68.65 ± 12.32
Height (cm)	172.62 ± 9.37

Table 1. Demographics of the dataset

Regarding the examination protocol, the longitudinal ultrasound scans of the bulkiest part of the medial head of the Gastrocnemius muscle were considered. Furthermore, a generous quantity of ultrasound gel (CLEAR ECO Supergel, Ceracarta S.p.A., Forli, Italy) was used to achieve the best possible ultrasound beam penetration and prevent deformation of the soft tissues, attributable to transducer pressure during the examination.

In total, 310 images from the 155 examinations were included in the evaluated dataset, randomly split (80%-20%) between the training and validation set with the well-established hold-out protocol. In particular, 244 images were selected as training set and 66 as validation, in which the results are reported. In addition, the annotation procedure of the deep and superficial aponeuroses was performed with the guidelines and overview of a specialised doctor. In Fig. 1, an image of GCM is presented along with their annotated aponeuroses.

To measure the muscle thickness, we follow the basic (MUSA) pipeline procedure described in [12]. It is known that the muscle thickness in the longitudinal plane is defined as the distance between the superficial and deep aponeuroses. Still, due to its variability along the longitudinal axis, it can be better approximated by cutting the muscle into a few sectors, computing each sector's distance and taking their mean value as output. For doing so, we initially drew two guidelines on the muscle contours to highlight the aponeuroses. Secondly, multiple connecting the two aponeuroses line segments are drawn and from their endpoints we calculate the distances. The average distance is the muscle thickness. The number of sectors is chosen to be five, and the procedure is illustrated in Fig. 1.

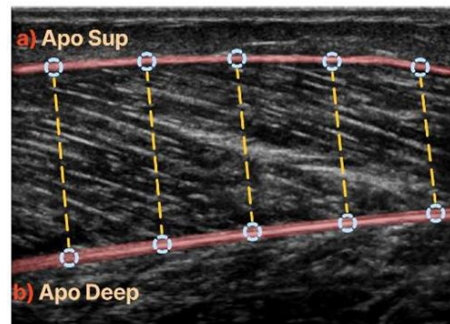


Figure 1: Annotation of the superficial (a) and deep (b) aponeuroses. The muscle thickness is measured from the average distance of the yellow dash lines.

2.2 Database

2.2.1 Introduction

Different state-of-the-art deep-learning architectures, used for automatically extracting the deep and superficial aponeuroses are presented in this section. In particular, UNet[18], Attention-UNet[14], UNet++[19] and UNeXt[20] have been incorporated for this task. These architectures have been recently applied successfully in different fields of medical segmentation. Our goal is to evaluate and compare them in the examined dataset of gastrocnemius medialis.

2.2.2 UNet

The UNet is maybe the most successful segmenter in recent years for its ability to be trained end-to-end with very few images. Its architecture consists of a contracting path to capture context and

a symmetric expanding path that enables precise localisation. Specifically, in the contracting path, network's input is repeatedly applied to two 3x3 convolutions, each followed by a rectified linear unit (ReLU) and a 2x2 max pooling operation with stride 2 for down sampling. Next, in the expansive path, an up-sampling of the feature map is applied, followed by a 2x2 convolution that halves the number of feature channels, a concatenation with the correspondingly cropped feature map from the contracting path, and two 3x3 convolutions, each followed by a ReLU. Finally, a 1x1 convolution maps each 64-component feature vector to the desired number of classes at the final layer.

2.2.3 Attention-UNet

The Attention-UNet is a variant of the original UNet architecture, boosted with attention gates to highlight better salient features passed through the skip connections. According to the authors, these attention gates can filter irrelevant and noisy responses in skip connections of the convolutional network. The above is performed before the concatenation operation to merge only relevant activations. Additionally, AGs filter the neuron activations during the forward pass as well as during the backward pass. Gradients originating from background regions are down-weighted during the backward pass, allowing model parameters in shallower layers to be updated, based mostly on spatial areas relevant to a given task.

2.2.4 UNet++

The UNet++ architecture is essentially a deeply-supervised encoder-decoder network where the encoder and decoder sub-networks are connected through a series of nested, dense skip pathways. The re-designed skip pathways aim at reducing the semantic gap between the feature maps of the encoder and decoder sub-networks. The underlying hypothesis behind the architecture is that the model can effectively capture fine-grained details of the foreground objects when high-resolution feature maps from the encoder network are gradually enriched before fusion with the corresponding semantically rich feature maps from the decoder network.

2.2.5 UNeXt

The UNeXt still follows a 5-layer deep encoder-decoder architecture of UNet with skip connections but changes the design of each block. In particular, a convolutional stage with a smaller number of filters in the initial and final blocks of the network, followed by an MLP stage, exists in UNeXt. In the bottleneck of the network, a novel Tokenized MLP is proposed which is effective at maintaining less computation burden, since it reduces the number of parameters significantly, while also maintaining a good performance.

2.2.6 Post-Processing

The prediction masks, that the deep learning architectures produce during inference, can contain artifacts. These artifacts are mostly small areas that do not belong to aponeuroses, but the segmentation networks falsely label them as so. Additionally, irregularities in the boundaries of the aponeuroses can also deteriorate the results. Both can be tackled by using image processing techniques. First, the contours of the structures of the prediction masks are extracted to remove the mislabeled areas, and only the two structures with the largest areas in terms of pixels are kept.

Furthermore, morphological operations are induced to improve the results for the boundary irregularities of aponeuroses.

2.2.7 Training Strategy

All the above-mentioned models were trained in the same fashion. In particular, the input of the networks was resized to be 256x256 with batch size 8 and number of epochs 300. The selected loss function was the Dice Loss, and an ADAM optimiser was used for the training process. Regarding the learning rate policy, a stepwise decrease of the learning rate was found best fitted. Furthermore, augmentation was performed for all the images during training with the following operations: vertical/horizontal flip, scaling, rotation and sharpening.

2.2.8 Evaluation Metrics

Several evaluation metrics were used to assess the proposed method's performance. First, regarding the image segmentation problem, five well-established indexes were incorporated [21]. Firstly, the Dice Coefficient (DSC) index, which measures the pixels overlap between two sets of data and secondly, (similarly to the DSC) the Intersection over Union (IoU) index. Furthermore, Precision and Recall of the segmentation maps were also reported between the manual and automatic measurements, as well as the Hausdorff distance (HD95) at the 95th percentile, which computes the highest distance between the two segmentation maps. Additionally, the mean discrepancy between the measurements was calculated in terms of the root mean square error (RMSE) in physical units (mm). Furthermore, the Intra-class Correlation Coefficient (ICC), type ICC (2, 1), and Pearson Correlation coefficient were used to evaluate the results statistically. Finally, Bland-Altman analysis was incorporated to evaluate possible bias and systematic error in the manual vs automatic muscle thickness measurements.

3. Results

Table 2 demonstrates the image segmentation task results for the four examined network topologies. In all the five metrics, the UNet exhibits superior performance in relevance with the other networks. In particular, the best reported Precision is 0.93, and the Recall is 0.84 showing the network's capability to accurately localise the deep and superficial aponeuroses. Furthermore, in terms of DSC the reported result equals 0.88, and the corresponding accuracy in HD95 is only 2.80, another indicator of the good performance of the segmented masks of the validation set.

	UNet	Att-UNet	UNet++	UNeXt
Precision	0.93 ± 0.05	0.92 ± 0.04	0.92 ± 0.05	0.92 ± 0.05
Recall	0.84 ± 0.05	0.84 ± 0.06	0.84 ± 0.05	0.81 ± 0.05
DSC	0.88 ± 0.03	0.88 ± 0.04	0.88 ± 0.03	0.86 ± 0.03
IoU	0.79 ± 0.05	0.78 ± 0.05	0.78 ± 0.05	0.76 ± 0.05
HD95	2.80 ± 1.46	4.47 ± 10.37	2.89 ± 1.68	3.59 ± 3.57

Table 2. Image Segmentation Metrics

Continuing our analysis, Table 3 compares the proposed method and a human operator for calculating muscle thickness. It presents the (mean ± standard deviations) for the muscle

thickness measurements and their discrepancy in RMSE and its reliability as measurement in terms of ICC metric.

Manual	Automatic	RMSE (mm)	ICC(2,1)
18.88 ± 2.30	18.82 ± 2.31	0.11 ± 0.11	0.99

Table 3. Muscle Thickness Measurements.

The evaluation results which have an extremely low RMSE and an ICC close to 1 in the evaluated dataset, are one more indicator of the usability of the proposed method for this task. It must also be highlighted that the difference between the proposed automated process and the measurements extracted from the operator is equal to 0.11 mm, a significant result that can be used for future automation of this clinical task.

Another useful analysis presented in Fig. 2 is the Bland-Altman plot of the muscle thickness measurements. The plot shows negligible additive bias since the mean value of all the readings is only 0.07 mm. Furthermore, the mean differences between the automatic and manual measurements of all the muscles are in the range of -0.20 – 0.34 mm. Most of the differences fall between the 95% limits of agreement. Finally, there are no distinguishable patterns depicted in the plots.

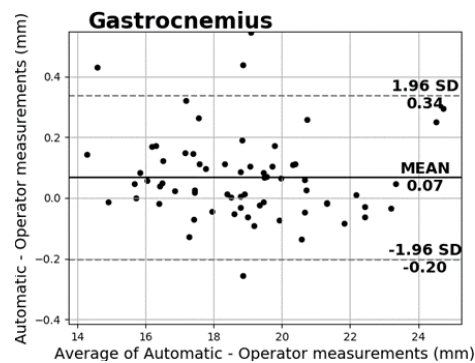


Figure 2: Bland-Altman Analysis of the manual vs automatic measurements.

Finally, in Fig. 3 qualitative results with the predictions of the network are presented. From the segmented masks, it is clear that the UNet can be applied effectively for automating the deep and superficial aponeuroses delineation.

4. Discussion

This study incorporated different state-of-the-art deep learning architectures to delineate the deep and superficial aponeuroses of ultrasound images of gastrocnemius medialis. The muscle thickness measurement was extracted from the segmented mask by taking the average distance in several endpoints across the muscle aponeuroses. Our preliminary results, extracted in the case of a very informative for the investigation of neuromuscular disorders and sarcopenia [7,22] muscle, indicate that such an automated approach can be used successfully in the clinical routine.

Regarding the clinical application of the results, it has been presented in [22] that a range in muscle thickness measurements of 5–10% is clinical relevant in the case of muscle hypotrophy

and a range above 10% in the case of severe neuromuscular disorders as sarcopenia. In our study, the average discrepancy between the automatic and manual measurements was equal to only 0.11 mm (under 0.01%), hence the results of the automatic process do not induce an error to these measurements, capable of leading to false diagnosis. Therefore, the proposed method is not only acceptable but also reliable to be integrated in the clinical routine as an additional diagnostic tool.

The usage of state-of-the-art deep learning architectures to delineate the muscle aponeuroses and later extract the muscle thickness, possess several advantages in relevance with the traditional gradient-based filtering methods, presented in [12,23]. Initially, deep learning approaches are less sensitive to noise, since during their learning process manage to distinguish the most relevant information to a given task. For example, in our problem, the UNet has managed to effectively separate the aponeuroses from the other muscle tissues existing nearby. Secondly, the proposed method is a purely data driven approach since it learns the best features directly from the input images. In contrast, designing a filter based approach from scratch, is a hard and tedious task that can lead to pure generalisation performance and overfitting. Hence, for these reasons we firmly believe that the proposed method can improve significantly the existing software investigation of neuromuscular disorders and sarcopenia [7,22] muscle, indicate that such an automated approach can be used successfully in the clinical routine.

Regarding the clinical application of the results, it has been presented in [22] that a range in muscle thickness measurements of 5–10% is clinical relevant in the case of muscle hypotrophy and a range above 10% in the case of severe neuromuscular disorders as sarcopenia. In our study, the average discrepancy between the automatic and manual measurements was equal to only 0.11 mm (under 0.01%), hence the results of the automatic process do not induce an error to these measurements, capable of leading to false diagnosis. Therefore, the proposed method is not only acceptable but also reliable to be integrated in the clinical routine as an additional diagnostic tool.

The usage of state-of-the-art deep learning architectures to delineate the muscle aponeuroses and later extract the muscle thickness, possess several advantages in relevance with the traditional gradient-based filtering methods, presented in [12,23]. Initially, deep learning approaches are less sensitive to noise, since during their learning process manage to distinguish the most relevant information to a given task. For example, in our problem, the UNet has managed to effectively separate the aponeuroses from the other muscle tissues existing nearby. Secondly, the proposed method is a purely data driven approach since it learns the best features directly from the input images. In contrast, designing a filter based approach from scratch, is a hard and tedious task that can lead to pure generalisation performance and overfitting. Hence, for these reasons we firmly believe that the proposed method can improve significantly the existing software. Although, the results presented here are encouraging, there are some limitations worth mentioning. One important limitation is that we examined only one muscle from over than 200 that the human body possess. Therefore, we cannot be fully confident about the generalisation ability of our algorithm in all of them. Another limitation factor is that all the ultrasound recordings have been acquired from the same machine and with the same settings. The alteration of this setup in real world scenarios, can lead to deterioration of the performance in a range that we have not evaluated. Nevertheless, since the results presented in this study have been produced with few hundred images, we strongly believe that, provided a sufficient number of training examples, these two limitations can be overcome.

Finally, as future work we plan to investigate the automatic extraction of muscle thickness measurement in more muscles and in a larger dataset of ultrasound images. Significantly, this dataset will consist of ultrasound recordings taken from young, healthy and elderly with pathological condition subjects. This more diverse and challenging dataset will provide us with a better understanding of the overall performance of the proposed method.

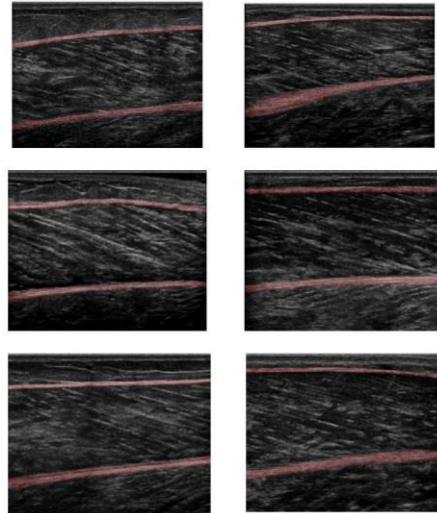


Figure 3 Qualitative results in images of Gastrocnemius medialis.

Acknowledgements

This research is co-financed by Greece and the European Union (European Social Fund- ESF) through the Operational Programme, “Human Resources Development, Education and Lifelong Learning” in the context of the project, “Strengthening Human Resources Research Potential via Doctorate Research” (MIS-5000432), implemented by the State Scholarships Foundation (IKY).

References

- [1] Franchi MV, Longo S, Mallinson J, Quinlan JI, Taylor T, Greenhaff PL, et al. Muscle thickness correlates to muscle cross-sectional area in the assessment of strength training-induced hypertrophy. *Scand J Med Sci Sports* 2018;28:846–53. <https://doi.org/10.1111/sms.12961>
- [2] Rieder F, Kösters A, Wiesinger H-P, Dorn U, Hofstaedter T, Fink C, et al. Alpine Skiing With total knee ArthroPlasty (ASWAP): muscular adaptations. *Scand J Med Sci Sports* 2015; 25:26–32. <https://doi.org/10.1111/sms.12451>
- [3] de Boer MD, Seynnes OR, di Prampero PE, Pišot R, Mekjavić IB, Biolo G, et al. Effect of 5 weeks horizontal bed rest on human muscle thickness and architecture of weight bearing and non-weight bearing muscles. *Eur J Appl Physiol* 2008;104:401–7. <https://doi.org/10.1007/s00421-008-0703-0>
- [4] Atkinson RA, Srinivas-Shankar U, Roberts SA, Connolly MJ, Adams JE, Oldham JA, et al. Effects of Testosterone on Skeletal Muscle Architecture in Intermediate-Frail and Frail Elderly Men. *J Gerontol Ser A* 2010;65A:1215–9. <https://doi.org/10.1093/gerona/glq118>
- [5] Agyapong-Badu S, Warner M, Samuel D, Narici M, Cooper C, Stokes M. Anterior thigh composition measured using ultrasound imaging to quantify relative thickness of muscle and non-contractile tissue: a potential biomarker for musculoskeletal health. *Physiol Meas* 2014;35:2165–76. <https://doi.org/10.1088/0967-3334/35/10/2165>

- [6] Pillen S, Arts IMP, Zwarts MJ. Muscle ultrasound in neuromuscular disorders. *Muscle Nerve* 2008;37:679–93. <https://doi.org/10.1002/mus.21015>
- [7] Barotsis N, Galata A, Hadjiconstanti A, Panayiotakis G. The ultrasonographic measurement of muscle thickness in sarcopenia. A prediction study. *Eur J Phys Rehabil Med* 2020; 56:427–37. <https://doi.org/10.23736/S1973-9087.20.06222-X>
- [8] Liu S, Wang Y, Yang X, Lei B, Liu L, Li SX, et al. Deep Learning in Medical Ultrasound Analysis: A Review. *Engineering* 2019;5:261–75. <https://doi.org/10.1016/j.eng.2018.11.020>
- [9] Marzola F, van Alfen N, Doorduyn J, Meiburger KM. Deep learning segmentation of transverse musculoskeletal ultrasound images for neuromuscular disease assessment. *Comput Biol Med* 2021; 135:104623. <https://doi.org/10.1016/j.compbiomed.2021.104623>
- [10] Salvi M, Caresio C, Meiburger KM, De Santi B, Molinari F, Minetto MA. Transverse Muscle Ultrasound Analysis (TRAMA): Robust and Accurate Segmentation of Muscle Cross-Sectional Area. *Ultrasound Med Biol* 2019;45:672–83. <https://doi.org/10.1016/j.ultrasmedbio.2018.11.012>
- [11] Karras T, Aittala M, Hellsten J, Laine S, Lehtinen J, Aila T. Training Generative Adversarial Networks with Limited Data. *ArXiv200606676 Cs Stat* 2020
- [12] Caresio C, Salvi M, Molinari F, Meiburger KM, Minetto MA. Fully Automated Muscle Ultrasound Analysis (MUSA): Robust and Accurate Muscle Thickness Measurement. *Ultrasound Med Biol* 2017;43:195–205. <https://doi.org/10.1016/j.ultrasmedbio.2016.08.032>
- [13] Katakis S, Barotsis N, Kakotaritis A, Economou G, Panagiotopoulos E, Panayiotakis G. Automatic Extraction of Muscle Parameters with Attention UNet in Ultrasonography. *Sensors* 2022;22:5230.
- [14] Oktay O, Schlemper J, Le Folgoc L, Lee M, Heinrich M, Misawa K, et al. Attention U-Net: Learning Where to Look for the Pancreas. 2018.
- [15] Barotsis N, Tsiganos P, Kokkalis Z, Panayiotakis G, Panagiotopoulos E. Reliability of muscle thickness measurements in ultrasonography. *Int J Rehabil Res Int Z Rehabil Rev Int Rech Readaptation* 2020; 43:123–8. <https://doi.org/10.1097/MRR.0000000000000390>
- [16] Katakis S, Barotsis N, Kastaniotis D, Theoharatos C, Tsiganos P, Economou G, et al. Muscle Type and Gender Recognition Utilising High-Level Textural Representation in Musculoskeletal Ultrasonography. *Ultrasound Med Biol* 2019;45:1562–73. <https://doi.org/10.1016/j.ultrasmedbio.2019.02.011>
- [17] Katakis S, Barotsis N, Kastaniotis D, Theoharatos C, Tsourounis D, Fotopoulos S, et al. Muscle Type Classification on Ultrasound Imaging Using Deep Convolutional Neural Networks. 2018 IEEE 13th Image Video Multidimens. Signal Process. Workshop IVMSWP, 2018, p. 1–5. <https://doi.org/10.1109/IVMSWP.2018.8448648>
- [18] Ronneberger O, Fischer P, Brox T. U-Net: Convolutional Networks for Biomedical Image Segmentation. *ArXiv150504597 Cs* 2015.
- [19] Zhou Z, Siddiquee MMR, Tajbakhsh N, Liang J. UNet++: A Nested U-Net Architecture for Medical Image Segmentation 2018. <https://doi.org/10.48550/arXiv.1807.10165>
- [20] Valanarasu JM, Patel VM. UNeXt: MLP-based Rapid Medical Image Segmentation Network 2022. <https://doi.org/10.48550/arXiv.2203.04967>
- [21] Bertels J, Eelbode T, Berman M, Vandermeulen D, Maes F, Bisschops R, et al. Optimizing the Dice Score and Jaccard Index for Medical Image Segmentation: Theory & Practice. vol. 11765, 2019, p. 92–100. https://doi.org/10.1007/978-3-030-32245-8_11
- [22] Minetto MA, Caresio C, Menapace T, Hajdarevic A, Marchini A, Molinari F, et al. Ultrasound-Based Detection of Low Muscle Mass for Diagnosis of Sarcopenia in Older Adults. *PM R*

- 2016;8:453–62. <https://doi.org/10.1016/j.pmrj.2015.09.014>
- [23] Salvi M, Caresio C, Meiburger KM, De Santi B, Molinari F, Minetto MA. Transverse Muscle Ultrasound Analysis (TRAMA): Robust and Accurate Segmentation of Muscle Cross-Sectional Area. *Ultrasound Med Biol* 2019;45:672–83.
<https://doi.org/10.1016/j.ultrasmedbio.2018.11.012>